Proceedings of the 20th International Conference on Soil Mechanics and Geotechnical Engineering– Rahman and Jaksa (Eds)

A three-dimensional non-orthogonal plastic flow rule for geomaterials

Dechun Lu, Jingyu Liang, Xin Zhou & Xiuli Du
Beijing University of Technology, 100 Pingleyuan, Chaoyang District, Beijing, China

ABSTRACT: In order to well capture the mechanical behavior of geomaterials, the non-associated plastic flow rule based on integer derivative is usually used to determine the plastic strain increment. Therefore, it is necessary to construct a potential function. However, it is difficult to derive an appropriate potential function directly from test results, and some additional parameters may be required. The non-orthogonal plastic flow rule is an alternative way, which determines the direction of the plastic strain increment by utilizing the non-orthogonal gradient of the yield function. The direction tensor of the plastic strain increment can be achieved by two steps: first, solve the fractional gradient of the yield function with respect to the stress invariants based on the fractional partial derivative, and then transform the fractional gradient into the ordinary stress space. These two steps overcome the difficulty that the existing chain rules of fractional derivative cannot be used directly. Based on the presented plastic flow rule, the framework of non-orthogonal elastoplastic constitutive model is thus established, which makes it possible for developing 3D elastoplastic constitutive models, and no potential function is used. The magnitude and direction of the plastic strain increment can be determined by the yield function and the hardening parameter. Based on the established model framework, 3D non-orthogonal elastoplastic models for soil and concrete are developed based on an ellipsoid yield function for soil and a closed-form yield function for concrete, respectively. Behaviors of soil and concrete under 3D stress conditions are well captured.

KEYWORDS: plastic flow direction; non-orthogonal plastic flow rule; elastoplastic model; granular material; concrete.

1 INTRODUCTION

The plastic flow rule is a kinematic hypothesis analogous to the orthogonality between the flow line and the plastic potential line. It gives a rule to be followed in determining the relative size and proportional relationship of the plastic strain increment, which can be expressed by the plastic flow direction. Since the Drucker plastic postulate was proposed, the associated plastic flow rule that the plastic potential function is chosen to be identical to the yield function, thereby establishing the relationship between the yield condition and the plastic constitutive relationship. The associated flow rule is usually taken as a simplified method for determining the direction of plastic strain increment (Roscoe & Burland, 1968; Sun *et al.*, 2004; Yao *et al.*, 2009; Borja & Choo, 2016). However, according to the experimental and theoretical studies, the associated plastic flow rule is unsuitable for geomaterials (Maier & Hueckel, 1979; Lade, 1988; Collins & Houlsby, 1997).

When the plastic potential function is newly constructed to be different from the yield function, the non-associated flow rule is adopted, and the plastic flow direction determined based on the orthogonal gradient of the plastic potential function is non-orthogonal to the yield surface (Yu *et al.*, 1999; Grassl, 2004; Xiao *et al.*, 2014; Wang *et al.*, 2018). The method based on the plastic potential function undoubtedly contributes to determining the non-orthogonal plastic flow direction. Nevertheless, an appropriate plastic potential function is hard to be directly constructed based on experimental results. On the other hand, the tedious work of constructing the plastic potential function complicates the establishment of the elastoplastic constitutive model, and may also bring some additional meaningless parameters (Krenk, 2000; Zhao & Gao, 2016; Lü *et al.*, 2018).

Actually, the purpose of constructing the plastic potential function is to obtain the plastic flow direction that is non-orthogonal to the yield surface. This mission can also be accomplished by the non-orthogonal gradient of the yield function based on the fractional derivative (Sumelka, 2014; Sun & Xiao, 2017; Lu *et al.*, 2019; Lu *et al.*, 2019; Sun & Sumelka, 2019). And simultaneously, the need to construct the plastic potential function can also be obviated. As a flexible mathematical tool that capable of generalizing the integer gradients to fractional gradients, the application of fractional differentiation in soil constitutive model is still in its initial stage.

In this paper, in view of the particularity of the fractional derivative, the covariant transformation is introduced, and the 3D non-orthogonal plastic flow rule is thus presented. On this basis, the framework of the 3D non-orthogonal elastoplastic (NOEP) constitutive model is developed. The yield function and the hardening parameter, which are two core elements of the NOEP model, are given for soil and concrete, respectively. Furthermore, the plastic flow direction and the plastic multiplier are derived, which contribute to the establishment of the NOEP model within the NOEP model framework. The established NOEP models for soil and concrete are also verified respectively.

2 A 3D NON-ORTHOGONAL PLASTIC FLOW RULE

Fractional derivative has been taken as a novel tool to extend classical plastic flow rule, and a fractional plastic flow rule has been proposed (Sumelka, 2014). The direction of the plastic strain increment was determined by the fractional partial derivative of the yield function with respect to σ_{ij}. However, for geomaterials, the yield function is commonly and conveniently expressed in terms of the stress invariants p, q, and θ. Different from the first order derivative, the chain rule of the fractional derivative is still in its exploring stage. Several expressions of the chain rule for fractional derivatives have been developed (Podlubny, 1998; Jumarie, 2013). Nevertheless, the proofs or counterexamples in the existing studies show that these fractional chain rules are only applicable to some special cases, and their mathematical rigor needs further verification. Due to these special characteristics of the fractional derivative, the fractional plastic flow rule can only be applied to the yield function that is expressed by σ_{ij}, such as the Huber-Miser-Hencky yield function (Sumelka & Nowak, 2016). Therefore, a plastic flow rule capable of determining the non-orthogonal plastic flow direction for geomaterils under 3D stress conditions is eagerly needed. For the yield function constructed by the stress invariants S_k in the S_{kl} coordinate system, the covariant transformation rather than the chain rule is used here, and the non-orthogonal plastic flow rule can thus be developed in two steps (Lu *et al.*, 2019): 1) First determine the non-orthogonal gradient $m_{kl}^{(S)}$ based on the fractional partial derivative of the yield function in the S_{kl} coordinate system. 2) Transform the non-orthogonal gradient in the S_{kl} coordinate system to the σ_{ij} coordinate system by the covariant transformation $\partial S_{kl}/\partial\sigma_{ij}$. The plastic strain increment can thus be obtained.

$$\mathrm{d}\varepsilon_{ij}^{\mathrm{p}} = \Lambda m_{ij}^{(\sigma)} = \Lambda \frac{\partial^{\mu} f}{\partial S_{kl}{}^{\mu}} \frac{\partial S_{kl}}{\partial \sigma_{ij}} \tag{1}$$

where Λ is the plastic multiplier, and m_{kl} (k, l=1, 2, 3) is the plastic flow direction.

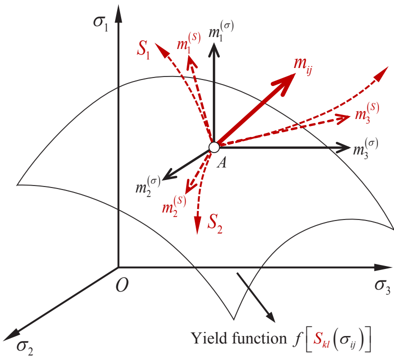

Figure 1 Schematic diagram of the non-orthogonal plastic flow rule.

The schematic diagram of the non-orthogonal plastic flow rule can be found in Figure 1. The superscripts (S) and (σ) for the components of m_{ij} in Figure 1 indicate that these components are in the S_{kl} and σ_{ij} coordinate system, respectively. The non-orthogonal plastic flow rule in tensor form is the kernel for determining the general expression of plastic strain increment, which is essential for the model implementation (Borja & Lee, 1990; Cui *et al.*, 2018). When the yield function is constructed based on the stress invariants (p, q, θ), the plastic strain increment in tensor form can thus be determined by the following equation:

$$\mathrm{d}\varepsilon_{ij}^{\mathrm{p}} = \Lambda\left(\frac{\partial^{\mu} f}{\partial p^{\mu}}\frac{\partial p}{\partial \sigma_{ij}} + \frac{\partial^{\mu} f}{\partial q^{\mu}}\frac{\partial q}{\partial \sigma_{ij}} + \frac{\partial^{\mu} f}{\partial \theta^{\mu}}\frac{\partial \theta}{\partial \sigma_{ij}}\right) \tag{2}$$

The proposed non-orthogonal plastic flow rule offers a novel view and a new approach to determine the plastic strain increment, and further provides the possibility for the establishment of a NOEP model for geomaterials. On the other hand, the plastic flow direction m_{ij} can also degenerate into the normal direction n_{ij} when μ=1.

3 FRAMEWORK OF THE 3D NOEP MODEL

Based on the elastoplastic theory, the total strain increment $\mathrm{d}\varepsilon_{ij}$ can be decomposed into two parts: the elastic strain increment $\mathrm{d}\varepsilon_{ij}^{\mathrm{e}}$ and the plastic strain increment $\mathrm{d}\varepsilon_{ij}^{\mathrm{p}}$. Therefore, we can get:

$$\mathrm{d}\varepsilon_{ij} = \mathrm{d}\varepsilon_{ij}^{\mathrm{e}} + \mathrm{d}\varepsilon_{ij}^{\mathrm{p}} \tag{3}$$

The elastic strain increment in Eq. (3) can be determined by the Hooke's law:

$$\mathrm{d}\varepsilon_{ij}^{\mathrm{e}} = \frac{1+\nu}{E}\mathrm{d}\sigma_{ij} - \frac{\nu}{E}\mathrm{d}\sigma_{kk}\delta_{ij} \tag{4}$$

where δ_{ij} is the Kronecker delta, ν is the Poisson's ratio. E is the Young's modulus, which can be determined based on the e-ln$p$ relationship of the swelling line.

$$E = 3\left(1-2\nu\right)\frac{1+e_0}{\kappa}p \tag{5}$$

where κ is the swelling index, and e_0 is the initial void ratio.

The plastic strain increment can be determined by the non-orthogonal plastic flow rule expressed in Eq. (1). The yield function and the hardening parameter are two key parts to determine the plastic strain increment. The yield surface is the equivalent surface of the hardening parameter, and its general form can be expressed as:

$$f = f\left[\sigma_{ij}, H\left(\varepsilon_{rt}^{\mathrm{p}}\right)\right] = 0 \tag{6}$$

where H is the hardening parameter indicating the hardening degree of soil due to the occurrence of plastic strain $\varepsilon_{rt}^{\mathrm{p}}$ (r, t=1, 2, 3). For geomaterials, the yield function can also be written as:

$$f = f\left[p, q, \theta, H\left(\varepsilon_{rt}^{\mathrm{p}}\right)\right] = 0 \tag{7}$$

The plastic flow direction m_{ij} in tensor form can thus be derived by applying the non-orthogonal plastic flow rule in Eq. (1) to the yield function in Eq. (7).

$$m_{ij} = \frac{\partial^{\mu} f}{\partial p^{\mu}}\frac{\partial p}{\partial \sigma_{ij}} + \frac{\partial^{\mu} f}{\partial q^{\mu}}\frac{\partial q}{\partial \sigma_{ij}} + \frac{\partial^{\mu} f}{\partial \theta^{\mu}}\frac{\partial \theta}{\partial \sigma_{ij}} \tag{8}$$

The plastic multiplier Λ can be determined based on the consistency condition, which is the total differential of the yield function:

$$\mathrm{d}f = \frac{\partial f}{\partial \sigma_{ij}}\mathrm{d}\sigma_{ij} + \frac{\partial f}{\partial H}\frac{\partial H}{\partial \varepsilon_{rt}^{\mathrm{p}}}\mathrm{d}\varepsilon_{rt}^{\mathrm{p}} = 0 \tag{9}$$

where $\varepsilon_{rt}^{\mathrm{p}}$ is the plastic strain used for constructing the hardening parameter H, and its increment can be expressed as $\mathrm{d}\varepsilon_{rt}^{\mathrm{p}} = \Lambda m_{rt}$. By substituting $\mathrm{d}\varepsilon_{rt}^{\mathrm{p}} = \Lambda m_{rt}$ into Eq. (9), the plastic multiplier Λ can be expressed as:

$$\Lambda = -\frac{\dfrac{\partial f}{\partial \sigma_{ij}}\mathrm{d}\sigma_{ij}}{\dfrac{\partial f}{\partial H}\dfrac{\partial H}{\partial \varepsilon_{rt}^{\mathrm{p}}}m_{rt}} \tag{10}$$

By substituting the plastic flow direction m_{ij} in Eq. (8) and the plastic multiplier Λ in Eq. (10) into Eq. (1), the plastic strain increment in the tensor form can be written as:

$$\mathrm{d}\varepsilon_{ij}^{\mathrm{p}} = \Lambda m_{ij} = -\frac{\dfrac{\partial f}{\partial \sigma_{kl}}\mathrm{d}\sigma_{kl}}{\dfrac{\partial f}{\partial H}\dfrac{\partial H}{\partial \varepsilon_{rt}^{\mathrm{p}}}m_{rt}}\left(\frac{\partial^{\mu} f}{\partial p^{\mu}}\frac{\partial p}{\partial \sigma_{ij}} + \frac{\partial^{\mu} f}{\partial q^{\mu}}\frac{\partial q}{\partial \sigma_{ij}}\right) \tag{11}$$

Finally, within the framework of the 3D NOEP model, the total strain increment can be determined by substituting Eqs. (4) and (11) into Eq. (3). As can be seen in this model framework, once the yield function and the hardening parameter are determined, the NOEP model can be established.

4 A 3D NOEP MODEL FOR SOIL

In order to make the NOEP model capable of reflecting the 3D properties of soil, the characteristic stress c_{ij} (Lu *et al.*, 2017) was proposed. By adopting this special stress concept, the yield function constructed by only two stress invariants can describe the mechanical behaviors of soil under 3D stress conditions (Ma *et al.*, 2017). The expression of the characteristic stress can be written as:

$$c_{ij}=p_r\left[\left(\frac{\sigma_1}{p_r}\right)^{\beta}n_i^{(1)}n_j^{(1)}+\left(\frac{\sigma_2}{p_r}\right)^{\beta}n_i^{(2)}n_j^{(2)}+\left(\frac{\sigma_3}{p_r}\right)^{\beta}n_i^{(3)}n_j^{(3)}\right] \quad (12)$$

where σ_k (k =1, 2, 3) is the principal stress, whose direction coincides with that of the ordinary principal stress. p_r is the reference stress, and the unit stress, like p_r=1kPa, is usually used. β is the characteristic stress index, which ranges from 0 to 1. $n_i^{(k)}$ is the directional cosine of the direction vector of the principal stress. Based on Eq. (12), the principal value of c_{ij} can be written as $c_k=p_r(\sigma_k/p_r)^{\beta}$. More details about the characteristic stress can be found in Lu *et al*. (Lu *et al.*, 2017; Liang *et al.*, 2020).

4.1 *Yield function and hardening parameter for soil*

In view of the superior abilities of c_{ij} in reflecting 3D properties of soil, the yield function can be expressed only based on two characteristic stress invariants c_n and c_s (Lu *et al.*, 2019). Here, the elliptical yield function similar to the yield function of the modified Cam-clay (MCC) model is used and can be expressed as:

$$f=c_s^2+\zeta^2F^2c_n^2-\zeta^2F^2c_nc_{nx}=0 \quad (13)$$

where ζF is the ratio of the vertical axis and the horizontal axis of elliptical yield curves, as shown in Figure 2. ζ is the shape parameter, and F is the failure stress ratio.

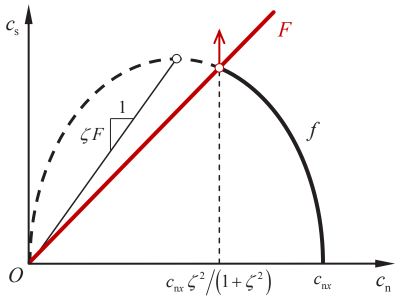

Figure 2 Possible shape of the yield curve.

Hardening parameter is an internal variable that reflects the hardening behaviors of soil during the loading process. It contributes to the determination of the plastic multiplier. As we all know, the plastic volumetric strain as a hardening parameter is effective for normally consolidated soil. And in order to describe the dilatancy behaviors of soil, a stress-path-independent factor Ω is introduced in the hardening parameter.

$$H=\int\Omega\mathrm{d}\varepsilon_v^p \quad (14)$$

According to the e-ln(c_n) line under isotropic compression conditions, the relationship $\varepsilon_v^p=l_p\ln c_{nx}/c_{n0}$ can be derived, where $l_p=(\lambda-\kappa)/[\beta\cdot(1+e_0)]$, and λ is the compression index. For soil with dilatancy, H is adopted to replace ε_v^p, therefore, c_{nx} can be expressed as:

$$c_{nx}=c_{n0}\exp\left(\frac{H}{l_p}\right) \quad (15)$$

Here, the hardening parameter capable of capturing the negative to positive dilatancy of soil during shear process is adopted (Liang *et al.*, 2020), which can be expressed as:

$$H=\int\frac{\mu\zeta^4F^4}{(2-\mu)F_f^4}\frac{\left(F_f^2-\chi^2\right)\left[(2-\mu)F_f^2+\mu\chi^2\right]}{\left(\zeta^2F^2+\chi^2\right)\left[\mu\zeta^2F^2-(2-\mu)\chi^2\right]}\mathrm{d}\varepsilon_v^p \quad (16)$$

4.2 *Plastic flow direction*

The plastic flow direction can be determined by applying the non-orthogonal plastic flow rule in Eq. (1) to the elliptical yield function in Eq. (13). In the process of solve the fractional partial derivative, the Caputo fractional derivative operator is used. Therefore, the non-orthogonal gradient of the yield function can be expressed as:

$$\left(\frac{\partial^{\mu}f}{\partial c_n{}^{\mu}},\frac{\partial^{\mu}f}{\partial c_s{}^{\mu}}\right)=\left(\frac{\mu N^2c_n^2+(\mu-2)c_s^2}{\Gamma(3-\mu)c_n^{\mu}},\frac{2c_s^{2-\mu}}{\Gamma(3-\mu)}\right) \quad (17)$$

Furthermore, the coordinate transformation coefficients $\partial c_n/\partial c_{ij}=\delta_{ij}/3$ and $\partial c_s/\partial c_{ij}=3/2\cdot(c_{ij}-c_n\delta_{ij})/c_s$ are introduced, and the plastic flow direction tensor m_{ij} can thus be obtained based on Eq. (1):

$$m_{ij}=\frac{\mu\zeta^2F^2c_n^2+(\mu-2)c_s^2}{\Gamma(3-\mu)c_n^{\mu}}\frac{\delta_{ij}}{3}+\frac{3c_s\left(c_{ij}-c_n\delta_{ij}\right)}{\Gamma(3-\mu)c_s^{\mu}} \quad (18)$$

With the expansion of the yield surface, the plastic flow directions under the condition of μ=0.52 and μ=1.00 are shown in Figure 3(a). The simple expression in Eq. (13) makes the yield surface in a simple shape of ellipsoid in the c_{ij} space, and it expands with only size changes. Correspondingly, the yield surface in the σ_{ij} space and its expansion are shown in Figure 3(b). The plastic flow directions for μ=0.52 and μ=1.00 determined by Eq. (18) are also shown in Figure 3(b). These figures show that the non-orthogonal plastic flow rule and the characteristic stress are complementary in describing soil behaviors under 3D stress conditions, and also give rise to a novel approach to capture the plastic flow direction for soil.

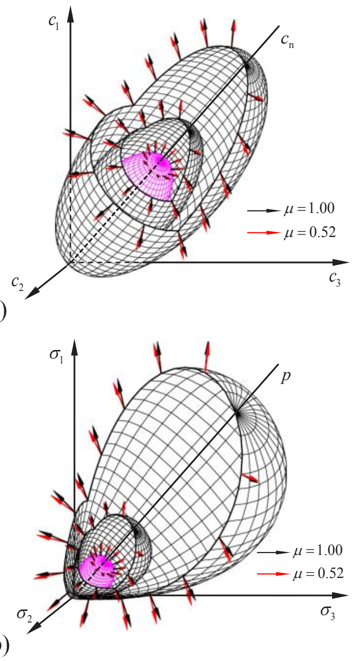

Figure 3 Evolution of the plastic flow direction with the expansion of the yield surface in: (a) the c_{ij} space; (b) the σ_{ij} space.

4.3 *Plastic multiplier*

According to Eq. (10), the plastic multiplier Λ in the c_{ij} space requires two item as follows:

$$\frac{\partial f}{\partial c_{ij}}\mathrm{d}c_{ij}=\zeta^2F^2\left(2c_\mathrm{n}-c_\mathrm{nx}\right)\mathrm{d}c_\mathrm{n}+2c_\mathrm{s}\mathrm{d}c_\mathrm{s} \tag{19}$$

$$\frac{\partial f}{\partial \varepsilon_\mathrm{v}^\mathrm{p}}=\frac{\partial f}{\partial c_\mathrm{nx}}\frac{\partial c_\mathrm{nx}}{\partial \varepsilon_\mathrm{v}^\mathrm{p}}=-\frac{\Omega}{l_\mathrm{p}}\zeta^2F^2c_\mathrm{n}c_\mathrm{nx} \tag{20}$$

By substituting Eqs. (19) and (20), together with Eq. (18) into the consistency condition in the c_{ij} space, the plastic multiplier Λ can be expressed as:

$$\Lambda=l_\mathrm{p}\Omega\frac{\Gamma\left(3-\mu\right)c_\mathrm{n}^{\mu}\left[\left(\zeta^2F^2c_\mathrm{n}^2-c_\mathrm{s}^2\right)\mathrm{d}c_\mathrm{n}+2c_\mathrm{s}c_\mathrm{n}\mathrm{d}c_\mathrm{s}\right]}{c_\mathrm{n}\left(c_\mathrm{s}^2+\zeta^2F^2c_\mathrm{n}^2\right)\left[\mu\zeta^2F^2c_\mathrm{n}^2+\left(\mu-2\right)c_\mathrm{s}^2\right]} \tag{21}$$

Within the framework of the NOEP model, once the plastic flow direction m_{ij} and the plastic multiplier Λ are derived, the plastic strain increment in the tensor form can be obtained based on Eq. (1). Together with the Hooke's law in Eq (4), the 3D NOEP model is established, which is capable of capturing the mechanical behaviours of soil under 3D stress conditions.

4.4 *Model verification*

The capability of the proposed NOEP model can be verified by the true triaxial drained test results (Nakai, 1989). Triaxial tests under p=196 when θ=15°, 30° and 45° are used here. The material parameters used for model prediction are $\lambda/(1+e_0)$= 0.00403, $\kappa/(1+e_0)$=0.00251, ν=0.3, φ=24.209°, φ_f=40.475°, β=0.24, ξ=2.3. Due to the contributions of the non-orthogonal plastic flow rule and the characteristic stress, the shear strength and relative proportional relationship among three principal strains are well captured, as shown in Figure 4 (a)~(c).

5 A 3D NOEP MODEL FOR CONCRETE

As the most widely used engineering construction materials, concrete will exhibit the significant dilatancy behavior under the shear load. For the finite element numerical analysis of concrete structure based on the plastic constitutive model, the traditional associated flow rule overestimates the volumetric expansion of material in compression, which will result in overestimating the strength of concrete in passive confinement. On the another hand, for the non-associated flow rule, the sophisticated plastic potential function and the pending model parameters have to be required, which creates additional difficulties in modeling of concrete material. The non-orthogonal flow rule (Lu *et al.*, 2019; Lu *et al.*, 2019) provides a new idea for describing the plastic deformation law of concrete material. In this section, the ability of non-orthogonal flow rules to describe dilatancy behavior of concrete is discussed and analyzed.

5.1 *Yield function and hardening parameter for concrete*

The concrete is a heterogeneous material composed of aggregates and cement matrix. There is the abundant micro-cracks and micro-voids in concrete and the plastic deformation mechanism of concrete is not only triggered by the shear load, but also by the hydrostatic load. Therefore, a closed form yield function is employed to capture plastic deformation behavior of concrete (Etse & Willam, 1994; Grassl *et al.*, 2013; Lu *et al.*, 2019).

$$f=\left[\left(1-H\right)\left(\frac{q}{3f_\mathrm{c}}-\frac{p}{f_\mathrm{c}}\right)^2+\frac{q}{f_\mathrm{c}}\right]^2+m_0H^2\left(\frac{q}{3f_\mathrm{c}}-\frac{p}{f_\mathrm{c}}\right)-H^2 \tag{22}$$

where f_c is the uniaxial compression strength. m_0 is the friction parameter and $m_0=f_\mathrm{c}/\sigma_0$. σ_0 is the three-dimensional tensile strength and a reference value $0.09f_\mathrm{c}$ can be used when σ_0 is not provided by test. H is a normalized hardening/softening function. When H increases to 1, Eq. (22) will degenerate into the quadratic function with respect to q and the yield surface in closed form will turn into the strength surface in open form as, as shown Figure 5. The expression of H can be expressed as follows:

$$H=\frac{Ax+(D-1)x^2}{1+(A-2)x+Dx^2} \tag{23}$$

where A and D are the shape parameters. $x=\varepsilon_\mathrm{d}^\mathrm{p}/\varepsilon_\mathrm{ds}^\mathrm{p}$ is the normalized internal variable and $\varepsilon_\mathrm{d}^\mathrm{p}=\sqrt{2/3\left(\varepsilon_{ij}-\varepsilon_\mathrm{v}^\mathrm{p}\delta_{ij}/3\right)\left(\varepsilon_{ij}-\varepsilon_\mathrm{v}^\mathrm{p}\delta_{ij}/3\right)}$. $\varepsilon_\mathrm{ds}^\mathrm{p}$ is the value of $\varepsilon_\mathrm{d}^\mathrm{p}$ at peak stress. The literature (Wang *et al.*, 2018) provides the calibration methods of A , D , and $\varepsilon_\mathrm{ds}^\mathrm{p}$.

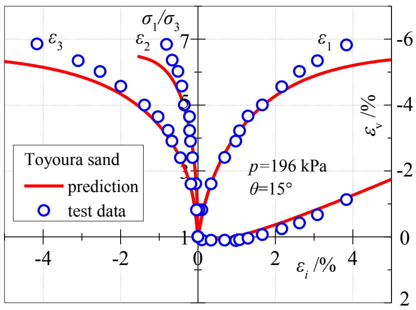

(a)

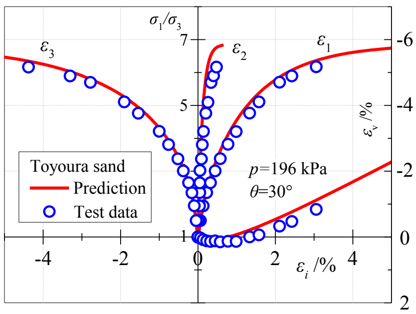

(b)

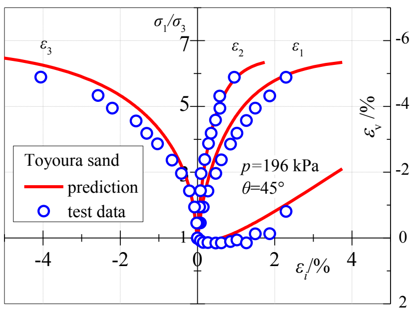

(c)

Figure 4 Comparison between predicted and test results.

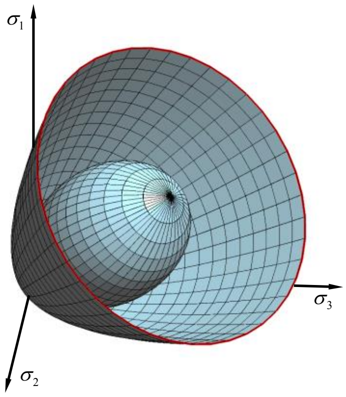

Figure 5. Open form strength surface and closed form yield surface

5.2 *Plastic flow direction*

Here, the RL fractional derivative is used to implement the non-orthogonal flow rule. Conducting the expansion operation to Eq. (22), the yield function can be rewritten the sums of power functions for *p* and *q* as follows

$$\begin{cases} f(p) = a_0 + a_1 \cdot p + a_2 \cdot p^2 + a_3 \cdot p^3 + a_4 \cdot p^4 \\ f(q) = b_0 + b_1 \cdot q + b_2 \cdot q^2 + b_3 \cdot q^3 + b_4 \cdot q^4 \end{cases} \tag{24}$$

where the fractional order μ can be determined by the method provided in the literature (Lu *et al.*, 2019; Zhou *et al.*, 2020).The coefficients a_k and b_k (k = 0, 1, 2, 3, 4) are:

$$\begin{cases} a_0(q) = \left[\dfrac{q}{f_c} + \dfrac{(1-H)q^2}{9f_c^2}\right]^2 + \dfrac{m_0 q r(\theta)H^2}{3f_c} - H^2 \\ a_1(q) = \dfrac{-4q^3(1-H)^2}{27f_c^4} - \dfrac{4(1-H)q^2}{3f_c^3} - \dfrac{m_0 H^2}{f_c} \\ a_2(q) = \dfrac{2(1-H)^2 q^2}{3f_c^4} + 2(1-H)\dfrac{q}{f_c^3} \\ a_3(q) = -\dfrac{4(1-H)^2 q}{3f_c^4} \\ a_4(q) = \dfrac{(1-H)^2}{f_c^4} \end{cases} \tag{25}$$

$$\begin{cases} b_0(p) = \dfrac{(1-H)^2 p^4}{f_c^4} - \dfrac{m_0 H^2 p}{f_c} - H^2 \\ b_1(p)\dfrac{-4(1-H)^2 p^3 + 6f_c(1-H)p^2}{3f_c^4} + \dfrac{m_0 r(\theta)H^2}{3f_c} \\ b_2(p) = \dfrac{2(1-H)^2 p^2 - 4f_c(1-H)p}{3f_c^4} + \dfrac{1}{f_c^2} \\ b_3(p) = \dfrac{2(1-H)}{9f_c^3} - \dfrac{4(1-H)^2 p}{27f_c^4} \\ b_4(p) = \dfrac{(1-H)^2}{81f_c^4} \end{cases} \tag{26}$$

Utilizing the properties of RL fractional derivative with respect to the power function (Lu *et al.*, 2019), the expressions for $\partial^\mu f / \partial p^\mu$ and $\partial^\mu f / \partial q^\mu$ can be obtained as follows:

$$\begin{cases} \dfrac{\partial^\mu f}{\partial p^\mu} = \dfrac{a_0 p^{-\mu}}{\Gamma(1-\mu)} + \dfrac{a_1\Gamma(2)p^{1-\mu}}{\Gamma(2-\mu)} + \dfrac{a_2\Gamma(3)p^{2-\mu}}{\Gamma(3-\mu)} + \dfrac{a_3\Gamma(4)p^{3-\mu}}{\Gamma(4-\mu)} + \dfrac{a_4\Gamma(5)p^{4-\mu}}{\Gamma(5-\mu)} \\ \dfrac{\partial^\mu f}{\partial q^\mu} = \dfrac{b_0 q^{-\mu}}{\Gamma(1-\mu)} + \dfrac{b_1\Gamma(2)q^{1-\mu}}{\Gamma(2-\mu)} + \dfrac{b_2\Gamma(3)q^{2-\mu}}{\Gamma(3-\mu)} + \dfrac{b_3\Gamma(4)q^{3-\mu}}{\Gamma(4-\mu)} + \dfrac{b_4\Gamma(5)q^{4-\mu}}{\Gamma(5-\mu)} \end{cases} \tag{27}$$

5.3 *Magnitude of plastic strain increment*

For the proposed non-orthogonal plastic model of concrete, the equivalent shear plastic strain ε_d^p is used as the plastic internal variable. The expression for the plastic multiplier Λ can be rewritten as follows:

$$\Lambda = -\frac{\dfrac{\partial f}{\partial \sigma_{ij}} \mathrm{d}\sigma_{ij}}{\dfrac{\partial f}{\partial H}\dfrac{\partial H}{\partial \varepsilon_d^p}\dfrac{\partial^\mu f}{\partial q^\mu}} \tag{28}$$

The gradient of yield function $\partial f / \partial \sigma_{ij}$ and the plastic internal variable gradient $\partial f / \partial \varepsilon_d^p$ can be obtained by the following steps:

$$\frac{\partial f}{\partial \sigma_{ij}} = \left(\frac{\partial f}{\partial p}, \frac{\partial f}{\partial q}\right)^T \left(\frac{\partial p}{\partial \sigma_{ij}}, \frac{\partial q}{\partial \sigma_{ij}}\right) \tag{29}$$

where $\partial f / \partial p$ and $\partial f / \partial q$ can be determined by:

$$\begin{cases} \dfrac{\partial f}{\partial p} = a_1 + 2a_2 p + 3a_3 p^2 + 4a_4 p^3 \\ \dfrac{\partial f}{\partial q} = b_1 + 2b_2 p + 3b_3 p^2 + 4b_4 p^3 \end{cases} \tag{30}$$

The expression of $\partial f / \partial \varepsilon_d^p$ can be obtained based on the chain law as follows:

$$\begin{aligned} \frac{\partial f}{\partial \varepsilon_d^p} &= \frac{\partial f}{\partial H}\frac{\partial H}{\partial \varepsilon_d^p} \\ &= \begin{Bmatrix} 2\left[(1-H)\left(\dfrac{q}{3f_c} - \dfrac{p}{f_c}\right)^2 + \dfrac{q}{f_c}\right]\left(\dfrac{q}{3f_c} - \dfrac{p}{f_c}\right)^2 \\ +2m_0 H\left(\dfrac{q}{3f_c} - \dfrac{p}{f_c}\right) - 2H \end{Bmatrix} \frac{\left[A(1+x) + 2(D-1)x\right](x-1)}{\varepsilon_{ds}^p\left[1 + (A-2)x + Dx^2\right]^2} \end{aligned} \tag{31}$$

5.4 *Model calibration*

In what follow, the ability of non-orthogonal flow rules to characterize the dilatancy behavior of concrete is analyzed based on the test data from Kupfer *et al.*, (1969). The model parameters are determined as $f_c = 32$ Mpa , $\sigma_0 = 2.88$ Mpa , $\varepsilon_{ds} = 0.0013$, $A = 9.26$, $D = 0.5$, $E = 32$ Gpa , $\nu = 0.2$. The different values of fractional order μ are used to evaluate the performance of non-orthogonal flow rule. Figure 6 shows the evolution law of plastic flow direction with different μ values on meridian plane and the comparison between model prediction with different μ values and test results. In plastic theory, the principal axis of plastic strain increment coincides with that of stress. The plastic flow direction on meridian plane is capable of characterizing the proportional relationship between plastic volume strain increment and plastic shear strain increment. It can be seen that, in the case of μ=1, the plastic flow direction perpendicular to the yield curve always points towards negative direction of p-axis, which leads to an overestimation of volume expansion phenomenon and cannot reasonably stress-strain behavior of concrete. By adjusting the value of μ, the different evolution law of plastic flow direction can be obtained. Especially, when μ equals to 1.984, the plastic flow direction can describe the volume change law from contraction to expansion. In this case, the stress-strain behavior of concrete is captured well by the non-orthogonal model.

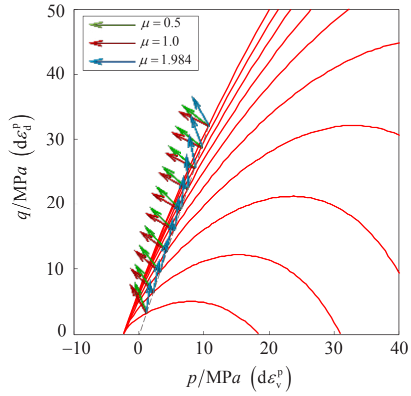

(a) Comparison of plastic flow direction

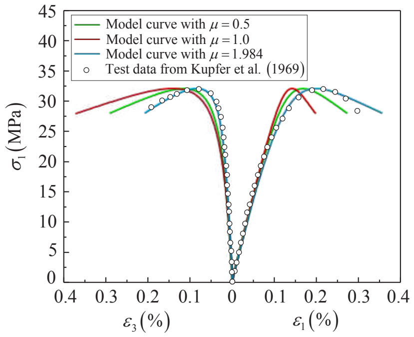

(b) Comparison of volume change law

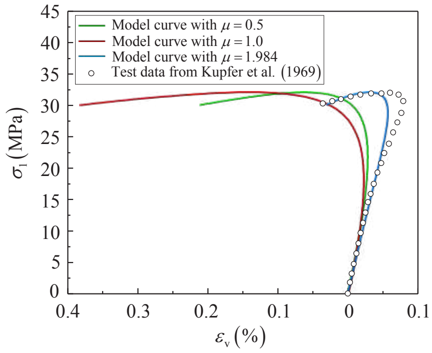

(c) Comparison of stress-strain relationship

Figure 6 Model analysis under different $m_0 = f_c/\sigma_0$ values (Test data from Kupfer et al., (1969))

6 CONCLUSIONS

This study aims to present a non-orthogonal plastic flow rule for geomaterials under 3D stress conditions. The non-orthogonal plastic flow rule provides a simple method for reproducing the complex deformation behaviors of geomaterials. Based on this, the framework of the 3D non-orthogonal elastoplastic model is developed. Within the framework of the non-orthogonal elastoplastic model, the constitutive model can be obtained only by specific expressions of the yield function and the hardening parameter. To characteristic the effect of the intermediate principal stress for soil under 3D stress conditions, the characteristic stress is employed, which helps to capture the soil behaviors under the 3D stress conditions. The elliptical yield function and a unified hardening parameter for soil is employed for developing a non-orthogonal elastoplastic model for soil. Moreover, a closed form yield surface and the unified form hardening/softening function are used as the basic elements for developing a non-orthogonal elastoplastic model for concrete. The plastic strain increment is determined from the perspective of the magnitude and direction. The former is calculated based on the consistency condition and latter is determined by the non-orthogonal flow rule. The comparison with the test data shows that the proposed non-orthogonal plastic models can well capture the mechanical behavior of soil and concrete, respectively.

7 ACKNOWLEDGEMENTS

This work was supported by the National Key Research and Development Program of China (Grant No. 2018YFC1504301) and the National Natural Science Foundation of China (Grant Nos. 51778026, 51421005 and U1839201).

8 REFERENCES

Borja, R.I., and Choo, J. (2016). Cam-Clay plasticity, Part VIII: A constitutive framework for porous materials with evolving internal structure. *Computer Methods in Applied Mechanics and Engineering*. 309, 653-679.

Borja, R.I., and Lee, S.R. (1990). Cam-Clay plasticity, Part I: Implicit integration of elasto-plastic constitutive relations. *Computer Methods in Applied Mechanics and Engineering*. 78, 49-72.

Collins, I.F., and Houlsby, G.T. Application of thermomechanical principles to the modelling of geotechnical materials., *Proceedings of the Royal Society of London. Series A: Mathematical, Physical and Engineering Sciences*, 1997, pp. 1975-2001.

Cui, W.J., Potts, D.M., Zdravković, L., Gawecka, K.A., and Taborda, D.M.G. (2018). An alternative coupled thermo-hydro-mechanical finite element formulation for fully saturated soils. *Computers and Geotechnics*. 94, 22-30.

Etse, G., and Willam, K. (1994). Fracture energy formulation for inelastic behavior of plain concrete. *Journal of Engineering Mechanics*. 120(9), 1983-2011.

Grassl, P. (2004). Modelling of dilation of concrete and its effect in triaxial compression. *Finite Elements in Analysis and Design*. 40(9-10), 1021-1033.

Grassl, P., Xenos, D., Nyström, U., Rempling, R., and Gylltoft, K. (2013). CDPM2: A damage-plasticity approach to modelling the failure of concrete. *International Journal of Solids and Structures*. 50(24), 3805-3816.

Jumarie, G. (2013). On the derivative chain-rules in fractional calculus via fractional difference and their application to systems modelling. *Central European Journal of Physics*. 11(6), 617-633.

Krenk, S. (2000). Characteristic state plasticity for granular materials Part I: Basic theory. *International Journal of Solids and Structures*. 37(43), 6343-6360.

Kupfer, H., Hilsdorf, H.K., and Rusch, H. (1969). Behavior of concrete under biaxial stresses. *Journal of the American Concrete Institute*. 66, 656-666.

Lade, P.V. (1988). Effects of voids and volume changes on the behaviour of frictional materials. *International Journal for Numerical and Analytical Methods in Geomechanics*. 12(4), 351-370.

Liang, J.Y., Lu, D.C., Du, X.L., Wu, W., and Ma, C. (2020). Non-orthogonal elastoplastic constitutive model for sand with dilatancy. *Computers and Geotechnics*. 118(103329), 1-11.

Lu, D.C., Liang, J.Y., Du, X.L., Ma, C., and Gao, Z.W. (2019). Fractional elastoplastic constitutive model for soils based on a novel 3D fractional plastic flow rule. *Computers and Geotechnics*. 105, 277-290.

Lu, D.C., Ma, C., Du, X.L., Jin, L., and Gong, Q.M. (2017). Development of a new nonlinear unified strength theory for geomaterials based on the characteristic stress concept. *International Journal of Geomechanics*. 17(2), 1-11.

Lu, D.C., Zhou, X., Du, X.L., and Wang, G.S. (2019). A 3D fractional elastoplastic constitutive model for concrete material. *International*

Journal of Solids and Structures. 165, 160-175.
Lü, X.L., Huang, M.S., and Qian, J.G. (2018). Influences of loading direction and intermediate principal stress ratio on the initiation of strain localization in cross-anisotropic sand. *Acta Geotechnica*. 13(3), 619-633.
Ma, C., Lu, D.C., Du, X.L., and Zhou, A.N. (2017). Developing a 3D elastoplastic constitutive model for soils: A new approach based on characteristic stress. *Computers and Geotechnics*. 86, 129-140.
Maier, G., and Hueckel, T. (1979). Nonassociated and coupled flow rules of elastoplasticity for rock-like materials. *International Journal of Rock Mechanics and Mining Sciences & Geomechanics Abstracts*. 16(2), 77-92.
Nakai, T. (1989). An isotropic hardening elastoplastic model for sand considering the stress path dependency in three-dimensional stresses. *Soils and Foundations*. 29(1), 119-137.
Podlubny, I. (1998). Fractional differential equations: an introduction to fractional derivatives fractional differential equations to methods of their solution and some of their applications. Academic Press.
Roscoe, K.H., and Burland, J.B. On the generalised stress-strain behaviour of 'wet' clay., *Engineering Plasticity*, Cambridge, England, 1968, pp. 535-609.
Sumelka, W. (2014). Fractional viscoplasticity. *Mechanics Research Communications*. 56, 31-36.
Sumelka, W., and Nowak, M. (2016). Non-normality and induced plastic anisotropy under fractional plastic flow rule: a numerical study. *International Journal for Numerical and Analytical Methods in Geomechanics*. 40(5), 651-675.
Sun, D.A., Matsuoka, H., Yao, Y.P., and Ishii, H. (2004). An anisotropic hardening elastoplastic model for clays and sands and its application to FE analysis. *Computers and Geotechnics*. 31(1), 37-46.
Sun, Y.F., and Sumelka, W. (2019). State-dependent fractional plasticity model for the true triaxial behaviour of granular soil. *Archives of Mechanics*. 71(1), 23-47.
Sun, Y.F., and Xiao, Y. (2017). Fractional order plasticity model for granular soils subjected to monotonic triaxial compression. *International Journal of Solids and Structures*. 118-119, 224-234.
Wang, G.S., Lu, D.C., Du, X.L., Zhou, X., and Cao, S.T. (2018). A true 3D frictional hardening elastoplastic constitutive model of concrete based on a unified hardening/softening function. *Journal of the Mechanics and Physics of Solids*. 119, 250-273.
Xiao, Y., Liu, H.L., Chen, Y.M., and Jiang, J.S. (2014). Bounding surface plasticity model incorporating the state pressure index for rockfill materials. *Journal of Engineering Mechanics*. 141(11), 1-15.
Yao, Y.P., Hou, W., and Zhou, A.N. (2009). UH model: three-dimensional unified hardening model for overconsolidated clays. *Géotechnique*. 59(5), 451-469.
Yu, M.H., Yang, S.Y., Fan, S.C., and Ma, G.W. (1999). Unified elasto-plastic associated and non-associated constitutive model and its engineering applications. *Computers and Structures*. 71, 627-636.
Zhao, J.D., and Gao, Z.W. (2016). Unified anisotropic elastoplastic model for sand. *Journal of Engineering Mechanics*. 142(1), 1-12.
Zhou, X., Lu, D.C., Du, X.L., Wang, G.S., and Meng, F.P. (2020). A 3D non-orthogonal plastic damage model for concrete. *Computer Methods in Applied Mechanics and Engineering*. 360, 112716.